Structural Analysis of a 50 cm Diameter Open-back Triangular Cell Beryllium Mirror in a Cryogenic Environment

Introduction

This paper discusses NASTRAN structural analysis of the Sub-Scale Beryllium Mirror Demonstrator (SBMD), which has been developed by Ball Aerospace as an experimental design concept for the Next Generation Space Telescope (NGST). The mirror was repeatedly subjected to 35K environment in the large cryogenic test chamber at Marshall Space Flight Center (MSFC). Deformations on the mirror surface were measured optically. The surface distortions predicted by NASTRAN are analyzed optically for comparison with the measured values. Model results compare favorably with measured results for ambient temperature validation cases. For the cryogenic environment case the influence of geometry and material property variations is being investigated to obtain closer correlation.

Model Description

The Beryllium mirror is a circular open-back triangular cell structure 532 mm in diameter. It has one flat side 266 mm long. A single face sheet serves as the mirror surface. The mirror surface is spherical with a 20 m radius of curvature. The open-back side of the mirror is flat. The depth or thickness at the center of the mirror is 50 mm. The triangular cells are equilateral triangles with a height of 76.5 mm (51 mm diameter inscribed circle). Some outer cells vary in shape. Mounting posts are located at some of the cell wall intersections. The tripod mounting holes are located at mid-span of a cell wall. All intersections have material removed for light-weighting. In addition all cell walls have material removed with rectangular cutouts. Beryllium (O-30) material properties are shown in Table I and the weight of the mirror is in Table II. Face sheet and cell wall thicknesses are shown in Table III. The mirror is represented with 8825 isoparametric quadrilateral plate elements, 20 triangular plate elements and 125 beam elements (mounting and non-mounting posts).

The tripod and bipods are titanium as are the fasteners that attach them to the mirror and Beryllium backplane. They are represented with beam elements. The material properties, weight and cross-sectional properties are shown in Tables I-III.

After model results were obtained with various load cases applied, it was determined that the Beryllium mirror model should be re-generated with a higher density finite element mesh. Several differences between the initial model and the drawing were noted and incorporated in the new model. The number of grid points within each triangular cell on the mirror surface increased from three to 61. These do not include the points at the intersections of the mirror surface and cell walls. The total number of grid points in the mirror model increased from 2055 to 9195. Points on the mirror surface increased from 572 to 5051. Results for numerous load cases were obtained and analysed for residual surface error.

It was shown in the briefing that a recent modification to the model significantly improved results to better agree with measured values. The modification involved the incorporation of the tripod and bipod mounting feet. The tripod flexure legs are offset from their bolted attachments by 12.7 mm long mounting feet. The bipod flexure legs are offset by approximately 20.83 mm. The incorporation of these feet introduced a bending moment in the cell walls which was not present before.

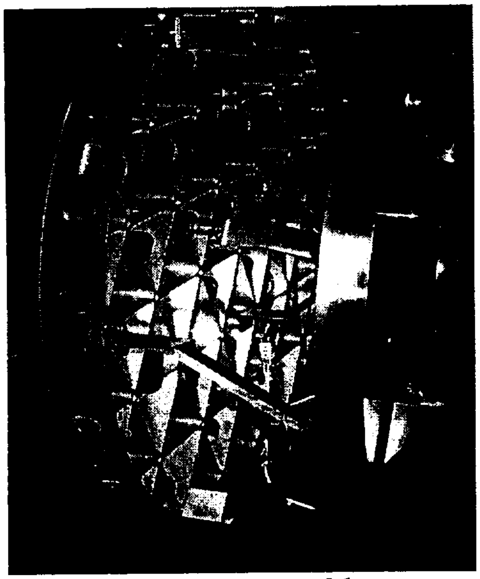

Figure 1. SBMD assembly mounted to backplane and test stand

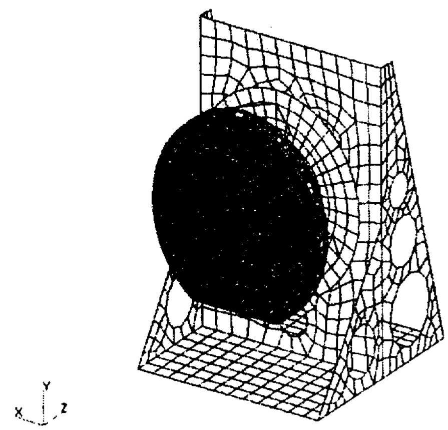

Figure 2. SBMD NASTRAN model

Table I Material properties

Name	Elastic Modulus, GPa	Poissons Ratio	Density, kg/m^3	CTE* ppm/K	Reference
Beryllium 0-30	289.58	0.1	1854.56	5.13	Ball model
Titanium Ti-6AL-4V	110.32	0.29	4428.8	6.75	Mil-Hdbk-5
Aluminum 5083-0	68.95	0.33	2768	15.3	Mil-Hdbk-5
Steel	206.84	0.29	8248.64	10.4	Mil-Hdbk-5

*Coefficient of thermal expansion (CTE) from ambient to 35K

Table II Mass Properties

Component	Material	Weight, kg
Mirror	Beryllium 0-30	2.009
Tripod	Titanium Ti-6AL-4V	0.2445
Bipods (3)	Titanium Ti-6AL-4V	0.676
Backplane	Beryllium 0-30	13.095
Mounting posts	Steel	0.2142
Stand	Aluminum 5083-0	55.25
Total		71.49

Table III Section Properties

Part Name	thickness, m	Area, m^2	I_1, m^4	I_2, m^4	J, m^4
mirror, face sheet	[redacted]				
mirror, cell walls	[redacted]				
backplane	[redacted]				
stand	[redacted]				
tripod feet		0.2559	0.0014	0.0213	0.00471
tripod flexures		0.05	1.042e-5	0.00417	4.167e-5
bipod feet		0.2559	0.0014	0.0213	0.00471
bipod flexures		0.05	0.00597	1.174e-5	4.7e-5
mirror, mounting posts		0.20694	0.00445	0.00445	0.0089
mirror, non-mounting posts		0.124	0.001962	0.001962	0.003925
mirror, big non-mounting posts		0.1736	0.005283	0.005283	0.010567
backplane mounting posts		0.019635	0.00307	0.00307	0.00614

Results

Model Validation

A force was applied to the model at the tripod apex and at ambient temperature. The force was directed towards and perpendicular to the mirror. The aluminum stand was constrained at its bottom surface. The model deformed as expected.

Figures 3 through 5 and 7 display PATRAN displacement and stress contour plots of the SBMD model and the mirror surface NASTRAN results. These are shown for information only and cannot be compared with measured results since no structural measuring devices (deflection or strain gages) were attached during testing.

The mirror residual surface error can be determined from the NASTRAN surface displacement results by representing the surface with Zernike polynomials and removing the respective error terms. These results can then be compared with measured test results. Figure 6 and figures 8-11 are residual surface error contour plots generated with Integrated Optical Design and Analysis (IODA) software developed for MSFC by SRS Technologies. The predicted values are compared with the measured values (Ref. 1) in Table IV.

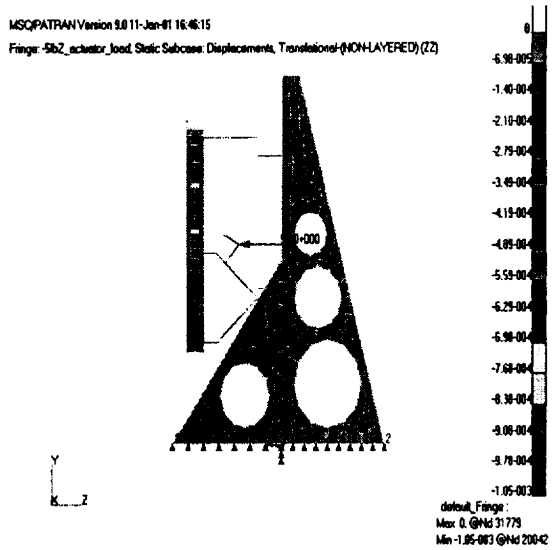

Figure 3. Contour fringe plot of Z-displacement (in) with applied load and boundary condition

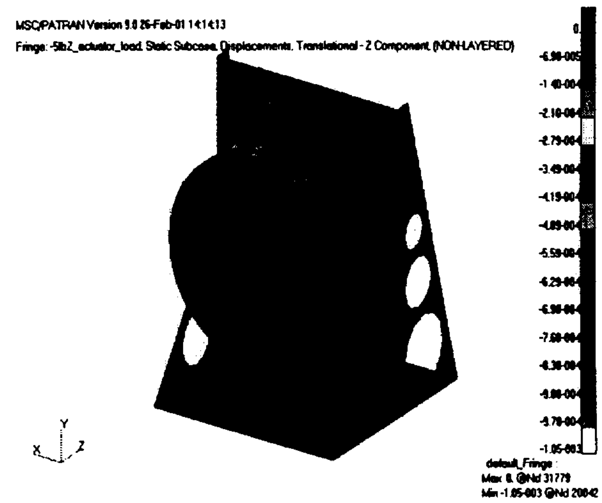

Figure 4. PATRAN Contour plot of Z-displacement (in.)

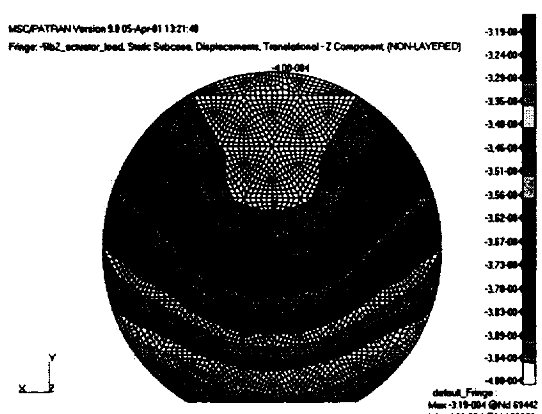

Figure 5. Mirror surface PATRAN contour plot of Z-displacement (in)

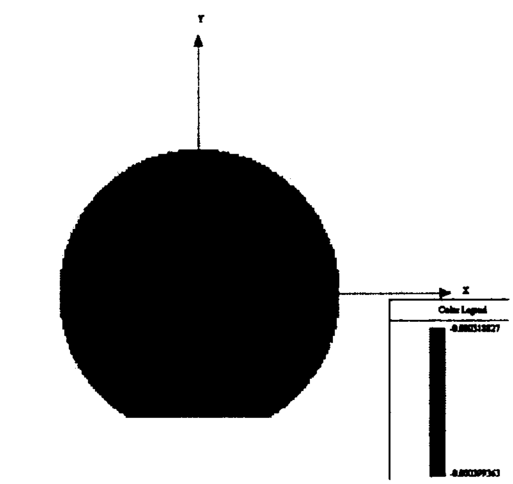

Figure 6. Zernike representation of mirror surface (no terms removed) Z-displacement (in)

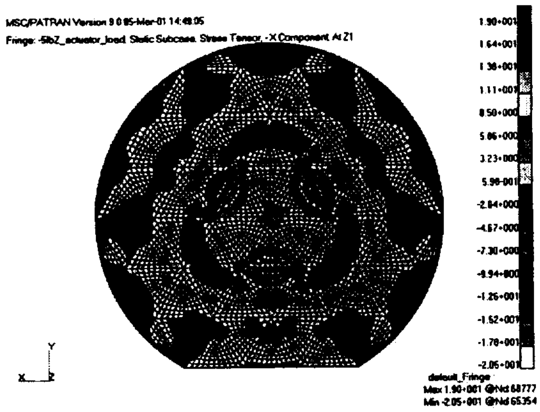

Figure 7. Mirror surface contour fringe plot of radial stress (psi)

Note the nearly identical mirror surface Z-displacement contour plots in Figures 5 and 6 (peak-to-valley magnitudes are identical). Figure 5 was produced with PATRAN directly from NASTRAN results and Figure 6 was generated with IODA which represents the surface with Zernike polynomials calculated from the NASTRAN displacement results. This similarity produces confidence in the software.

The effect of the tripod on the mirror surface stress is clearly evident in Figure 7. It is also interesting to note the similarity between radial stress contour fringes and the residual surface error contours in Figure 11.

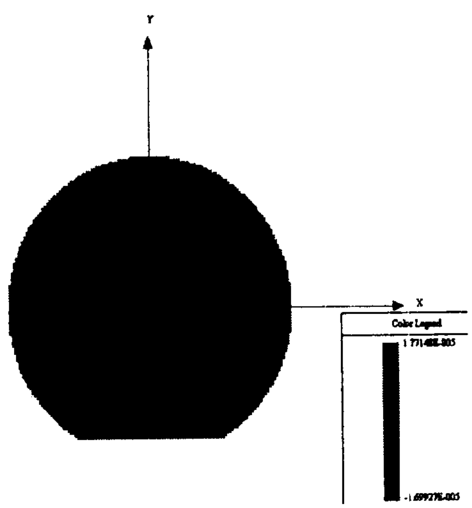

Figure 8. Mirror surface plot with tip, tilt and piston removed (in)

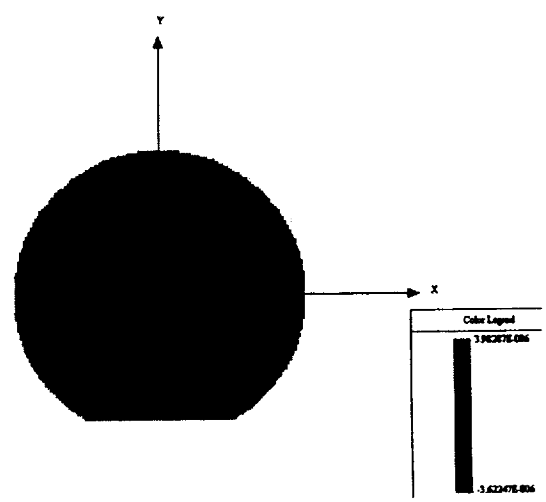

Figure 9. Mirror surface plot with Piston, tip, tilt and power removed (in)

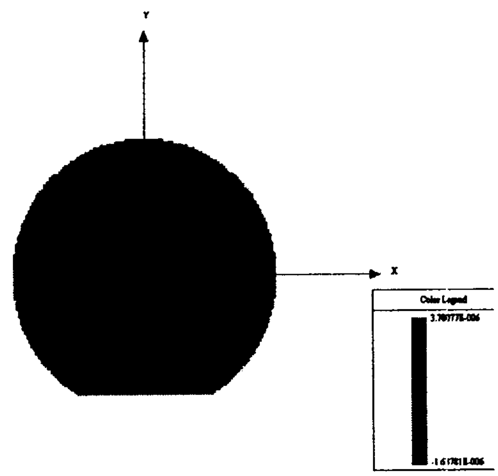

Figure 10. Mirror surface plot with 36 Zernike terms removed (in)

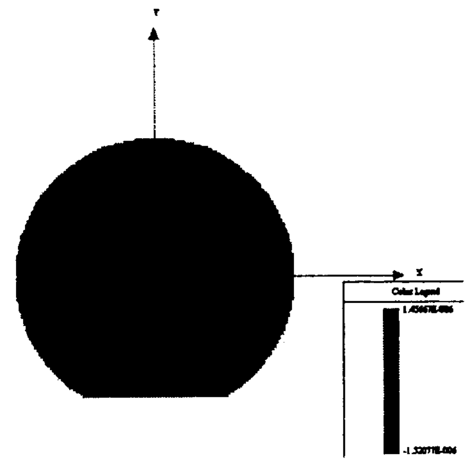

Figure 11. Mirror surface plot with 42 Zernike terms removed (in)

Table IV Comparison of Measured and Analytical Results

Zernike terms removed	Measured rms (μm)	Predicted rms (μm)	Measured P-V (μm)	Predicted P-V (μm)
Piston, tip,tilt	0.1587	0.227	0.6261	0.83
Piston, tip, tilt, power	0.0483	0.043		0.193
First 42	0.0051	0.008	0.0404	0.076

A vertical 1G gravity load was applied to the structure to further validate the model. The aluminum test stand was constrained in the same manner. The structure deformed as expected. Results are shown in figures 12- 17 and compared to measured results in Table V.

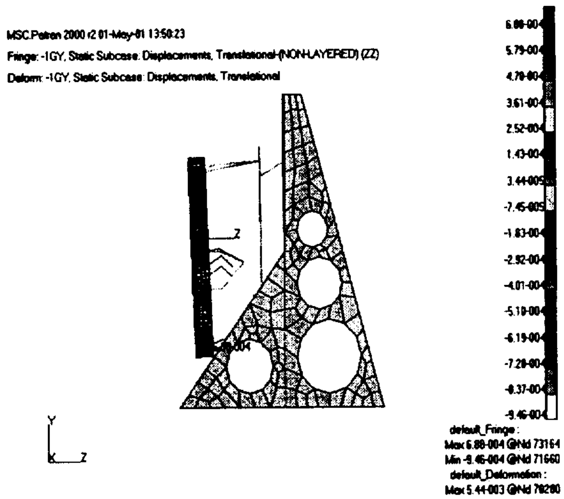

Figure 12. PATRAN contour plot of Z-displacement (in)

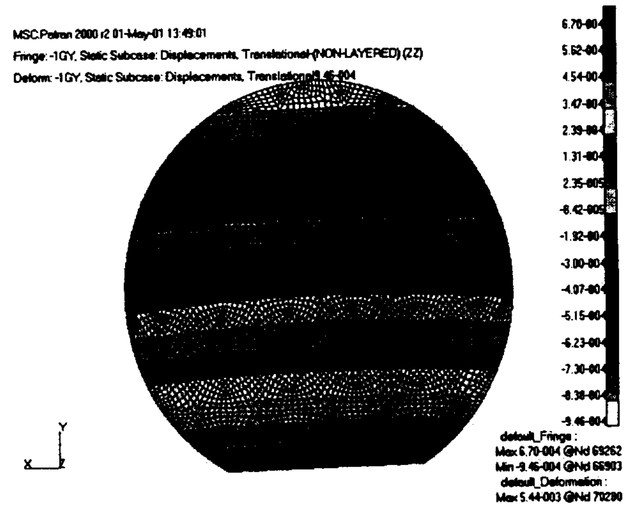

Figure 13. Mirror surface PATRAN contour plot of Z-displacement (in)

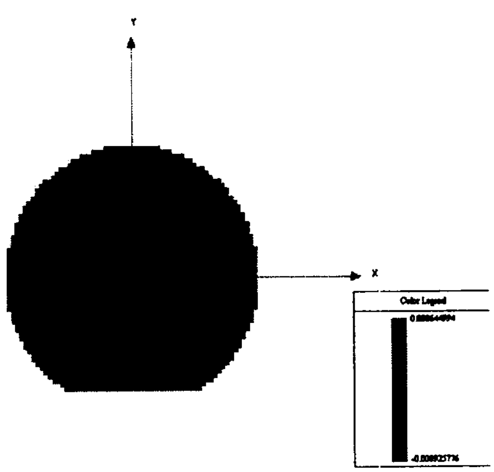

Figure 14. Zernike representation of mirror surface (no terms removed) Z-displacement (in)

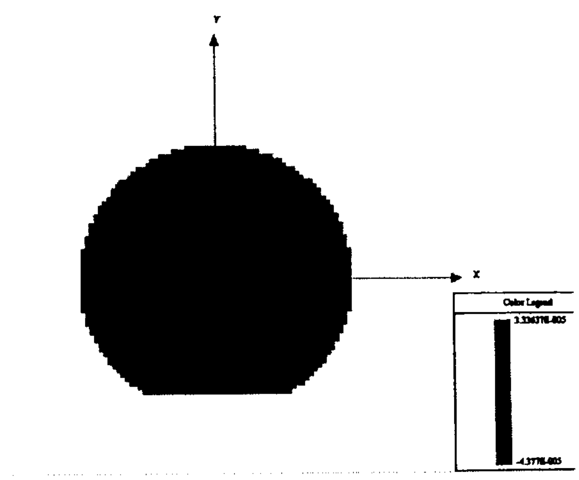

Figure 15. Mirror surface plot with tip, tilt and piston removed (in)

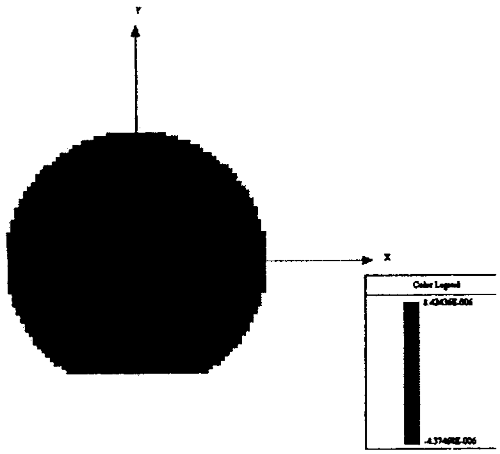

Figure 16. Mirror surface plot with piston, tip, tilt, power and astigmatism removed (in)

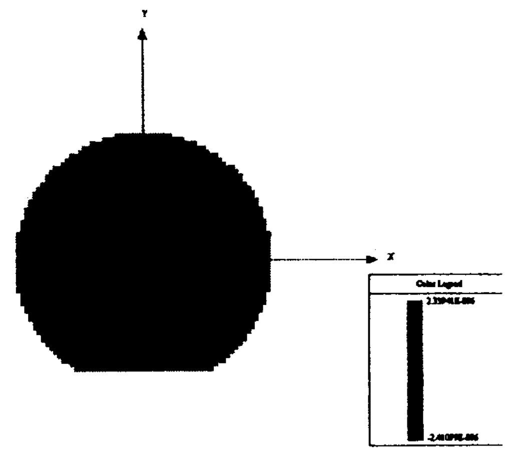

Figure 17. Mirror surface plot with 36 Zernike terms removed (in)

Table V Comparison of Measured and Analytical Results

Zernike terms removed	Measured rms (μm)	Predicted rms (μm)	Measured P-V (μm)	Predicted P-V (μm)
Piston, tip,tilt	0.329	0.440	2.397	2.023
Piston, tip, tilt, power, astigmatism	0.0287	0.046	0.1949	0.337
First 36	0.0083	0.0125	0.123	0.124

Ambient to 30K

The SBMD model was subjected to a single thermal load consisting of a 30K uniform temperature environment (–263K delta T or 293K minus 30K) with the aluminum test stand constrained as described above. Nominal CTE values for all materials were used. The model deformed structurally as expected. NASTRAN results are shown in Figures 12-15.

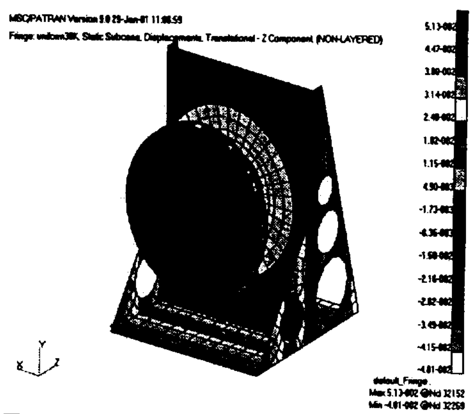

Figure 18. SBMD model Z-displacement (in)

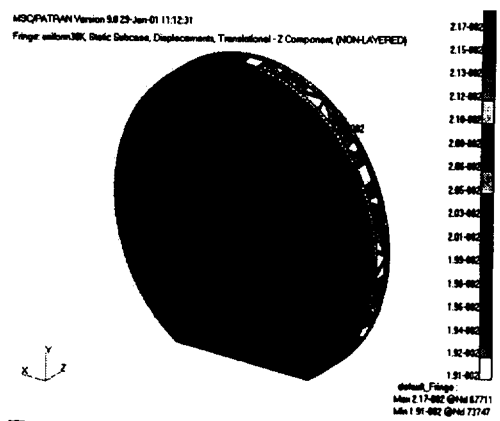

Figure 19. SBMD mirror model Z-displacement (in)

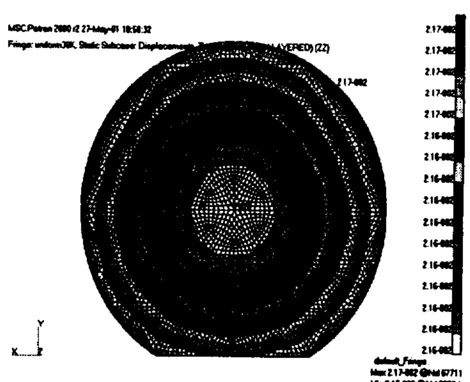

Figure 20. SBMD mirror surface model Z-displacement (in)

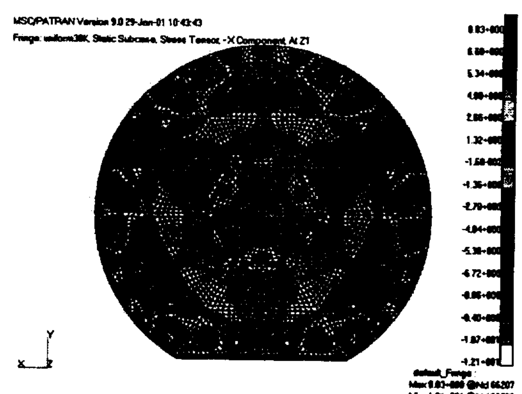

Figure 21. SBMD mirror surface model radial stress (psi)

The effect of the tripod and bipods on mirror surface stress is clearly seen in Figure 21. The contours and magnitudes generated by NASTRAN in Figure 20 should be very similar to those in Figure 22 produced by the Zernike representation shown in Figure 22.

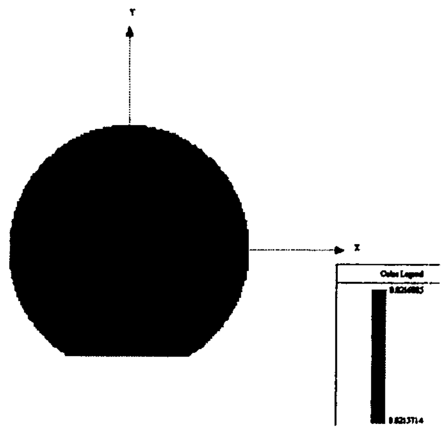

Figure 22. Zernike representation of mirror surface (no terms removed) Z-displacement (in)

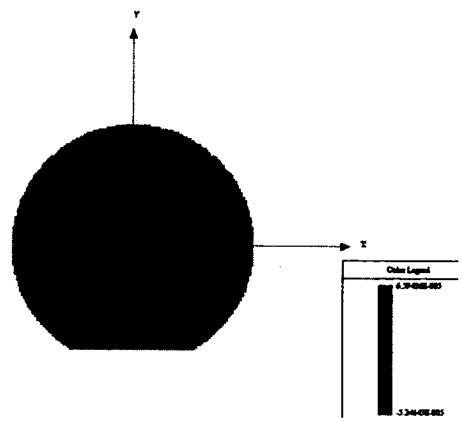

Figure 23. Mirror surface, piston, Tip, and tilt removed

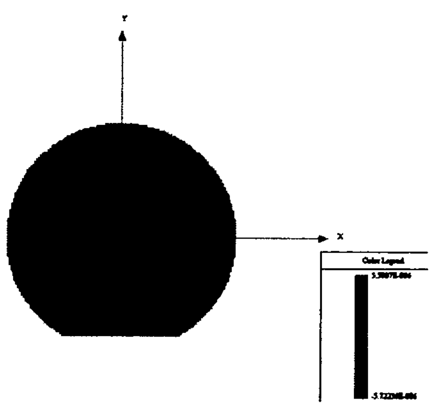

Figure 24. Mirror surface, piston, Tip, tilt and power removed

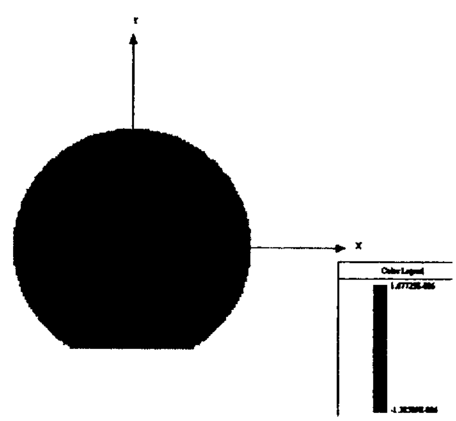

Figure 25. Mirror surface first 42 Zernike terms removed

Table V Comparison of Measured and Analytical Results

Zernike terms removed	Measured rms (μm)	Predicted rms (μm)	Measured P-V (μm)	Predicted P-V (μm)
Piston, tip,tilt	0.294	0.762	2.271	3.0
Piston, tip, tilt, power	0.062	0.051	0.571	0.287
First 42	0.012	0.009	0.134	0.078